Kobe University Repository : Kernel

PDF issue: 2025-12-05

Crystal Architectures and Magnetic Properties of Alkylferrocenium Salts with FnTCNQ (n = 0, 2, 4): Effect of Substituents on the Self-Assembled Structures

Mochida, Tomoyuki
Akasaka, Takahiro
Funasako, Yusuke
Nishio, Yutaka
Mori, Hatsumi

(Citation)
Crystal growth & design,13(10):4460-4468

(Issue Date)
2013-10

(Resource Type)
journal article

(Version)
Accepted Manuscript

(URL)
https://hdl.handle.net/20.500.14094/90002149

KOBE UNIVERSITY

Crystal Architectures and Magnetic Properties of Alkylferrocenium Salts with F_nTCNQ (n = 0, 2, 4): Effect of Substituents on the Self-assembled Structures

Tomoyuki Mochida,[†,‡] Takahiro Akasaka,[†,‡] Yusuke Funasako,[†] Yutaka Nishio,[§] and Hatsumi Mori[¶]*

[†]Department of Chemistry, Graduate School of Science, Kobe University, Kobe, Hyogo 657-8501, Japan

[‡]Department of Chemistry, Faculty of Science, Toho University, Miyama, Funabashi, Chiba 274-8510, Japan

[§]Department of Physics, Faculty of Science, Toho University, Miyama, Funabashi, Chiba 274-8510, Japan

[¶]Institute for Solid State Physics, The University of Tokyo, Kashiwanoha, Kashiwa, Chiba 277-8581, Japan

ABSTRACT: The crystal architecture and magnetic properties of the alkylferrocenium salts of tetracyanoquinodimethane (TCNQ) type acceptors have been investigated using 1,1′-dimethyl-, 1,1′-diethyl-, 1,1′-diisopropyl-, *tert*-butyl-, and *tert*-pentyl-ferrocene as the donors. In all of the resulting salts, the donors and acceptors were stacked to form independent columns. The F_4TCNQ salts had a D/A ratio of 1:1, and existed as hexagonal assembled structures composed of anion columns surrounded by cation columns. The F_2TCNQ and TCNQ salts had a D/A ratio of 1:2, and existed as a rectangular arrangement of cation columns. Weak antiferromagnetic interactions were found to operate between the cations in these salts.

INTRODUCTION

The crystal engineering of supramolecular organometallic materials including metallocene-based salts has become an important area of research in recent years.[1–3] Metallocene-based charge-transfer (CT) salts have also attracted attention because of their solid state electronic properties such as their magnetism and electrical conductivities.[4-6] A wide variety of different CT salts have been synthesized to date composed of ferrocene-type donors and organic acceptors, including tetracyanoethylene, tetracyanoquinodimethane (TCNQ) derivatives, and metal dithiolates. The assembled structures of these salts are typically composed of an alternate donor–acceptor arrangement as well as a segregated-stack arrangement, and the packing structures of these structures are critical to the bulk electronic properties of the salts. Based on our own interest in the crystal engineering of ferrocene-based CT salts, we previously reported the crystal architectures and magnetic properties of a series of alkylferrocenium salts with the $[Ni(mnt)_2]$ anion[7] (mnt = maleonitriledithiolato). These salts existed as hexagonal supramolecular assembled structures of alkylferrocenium cations, which surrounded the anion.

In this study, the crystal structures of the alkylferrocenium salts with TCNQ derivatives have been investigated. To evaluate the effect of different substituents on the assembled structures, 1,1′-dimethyl-, 1,1′-diethyl-, 1,1′-diisopropyl-, *tert*-butyl-, and *tert*-pentyl-ferrocene were used as the donors (abbreviated as Me_2fc, Et_2fc, $^{i}Pr_2$fc, ^{t}BuFc, and ^{t}PeFc, respectively, hereafter), and F_nTCNQ (n = 0, 2, and 4) as the acceptors (Chart 1). The electron affinity of the F_nTCNQ acceptor can be controlled by changing the number of the fluorine atoms [e.g., $E_{1/2}$ = 0.22 V (TCNQ), 0.41 V (F_2TCNQ), and 0.60 V (F_4TCNQ), in CH_3CN, *vs.* SCE],[8] and their use in CT complexes has been well documented.[9] Our previous study of biferrocenium salts revealed that F_4TCNQ and TCNQ afforded salts with different

D/A ratios.[10] Herein, we report the crystal structures and magnetic properties of alkylferrocenium salts **1**–**9** shown in Chart 2. Furthermore, the crystal structure of $(Me_2fc)(TCNQ)_2$ (**9**)[11] has been redetermined. The results of the current study revealed that the D/A ratios and assembled structures were strongly dependent on the acceptors. The intermolecular magnetic interactions between the cations have also been discussed.

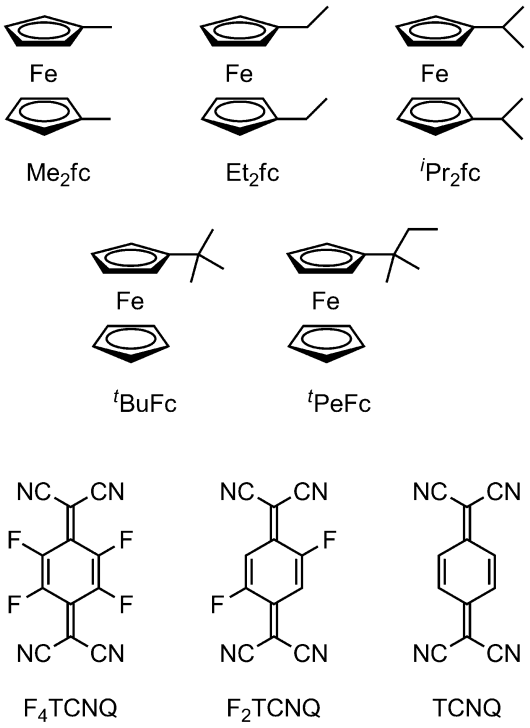

Chart 1

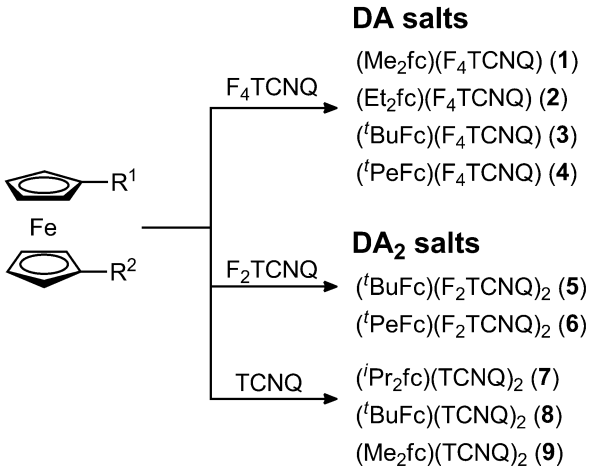

Chart 2

EXPERIMENTAL SECTION

General. Infrared spectra were recorded on a SHIMADZU Prestige-21 FTIR-8400S spectrometer equipped with an AIM-8800 microscope operating in the 4000–400 cm^{-1} range. The magnetic susceptibilities were measured using a Quantum Design MPMS–2 SQUID susceptometer at temperatures in the range of 2 to 300 K at a constant field of 5000 G. The diamagnetic contribution to the magnetic susceptibility was calculated using Pascal's law. Intermolecular overlap integrals between the LUMO orbitals of the acceptors were calculated based on the extended Hückel molecular orbital method.[12] The molecular volumes of the cations and anions were estimated using Spartan '10 software (Wavefunction Inc.)[13] on the crystallographically determined molecular structures. Calorimetric measurements of the single crystals of **6** and **7** were conducted using a differential thermal analysis (DTA) method[14] for samples less than 0.3 mg, and recorded during the heating process at a scan rate of 20 mK s^{-1}. The temperatures of the thermal bath and the samples were measured using a Cernox resistance thermometer and a chromel-constantan thermocouple with a diameter of 25 mm, respectively. Polystyrene (NIST SRM705a) pellets were used as a reference sample.

Preparation of charge-transfer salts. F_2TCNQ was prepared by the literature method.[15] $(Me_2fc)(TCNQ)_2$ (**9**) was prepared by a method different from the literature.[11] Other reagents and solvents were commercially available. The salts were obtained as single components.

Single crystals of $(Me_2fc)(F_4TCNQ)$ (**1**), (^{t}BuFc)(F_4TCNQ) (**3**), and (^{t}PeFc)(F_4TCNQ) (**4**) were prepared as follows. A solution of the donor (0.021 mmol) in $CHCl_3$ (1 mL), a mixture of $CHCl_3$ and CH_2Cl_2 (1:1, 2 mL), and a solution of F_4TCNQ (0.020 mmol) in CH_2Cl_2 (4 mL) were carefully layered in a test tube and allowed to diffuse for a week. Black crystals precipitated, which were suitable for X-ray crystallography. **1**: Yield: 63%. Anal. Calcd. for $C_{24}H_{14}F_4FeN_4$ (490.23): C, 58.80; H, 2.88; N, 11.43. Found: C, 58.68; H, 2.79; N, 11.44. ν (cm^{-1}) = 3045, 2196 (CN), 2177 (CN), 1630, 1537, 1499, 1479, 1389, 1348, 1339, 1263,

1198, 1144, 1051, 1026, 970, 895, 847. **3**: Yield: 71%. Anal. Calcd. for $C_{26}H_{18}F_4FeN_4$ (518.29): C, 60.25; H, 3.50; N, 10.81. Found: C, 60.24; H, 3.47; N, 10.80. ν (cm^{-1}) = 3096, 2967, 2201 (CN), 2178 (CN), 1634, 1539, 1501, 1391, 1344, 1267, 1200, 1146, 974, 872, 853, 789, 718. **4**: Yield: 86%. Anal. Calcd. for $C_{27}H_{20}F_4FeN_4$ (532.31): C, 60.92; H, 3.79; N, 10.53. Found: C, 61.04; H, 3.79; N, 10.51. ν (cm^{-1}) = 3086, 2979, 2192 (CN), 2176 (CN), 1630, 1534, 1499, 1383, 1342, 1266, 1197, 1145, 971, 853.

Single crystals of (Et_2fc)(F_4TCNQ) (**2**), (^{t}BuFc)(F_2TCNQ)$_2$ (**5**), and (^{t}PeFc)(F_2TCNQ)$_2$ (**6**) were prepared as follows. A mixture of donor (0.021 mmol for **2**, 0.10 mmol for **5** and **6**) and acceptor (0.020 mmol for **2**, 0.040 mmol for **5** and **6**) was dissolved in CH_2Cl_2 (4–6 mL), and vapor of diethyl ether or pentane was diffused into this solution. Black crystals precipitated in a few days, which were suitable for X-ray crystallography. **2**: Yield: 83%. Anal. Calcd. for $C_{26}H_{18}F_4FeN_4$ (518.29): C, 60.25; H, 3.50; N, 10.81. Found: C, 60.21; H, 3.45; N, 10.76. ν (cm^{-1}) = 3117, 3102, 2972, 2940, 2201 (CN), 2181 (CN), 1630, 1535, 1501, 1476, 1435, 1389, 1348, 1337, 1312, 1263, 1202, 1142, 1051, 970, 905, 893, 868, 860, 847, 787, 716. **5**: Yield: 55%. Anal. Calcd. for $C_{38}H_{22}F_4FeN_8$ (722.47): C, 63.17; H, 3.07; N, 15.51. Found: C, 63.32; H, 3.01; N, 15.51. ν (cm^{-1}) = 3093, 2183(CN), 2169(CN), 1606, 1530, 1514, 1485, 1365, 1346, 1243, 1207, 1182, 1151, 858, 850, 790, 685, 564, 554. **6**: Yield: 49%. Anal. Calcd. for $C_{39}H_{24}F_4FeN_8$ (736.50): C, 63.60; H, 3.28; N, 15.21. Found: C, 63.80; H, 3.24; N, 15.21. ν (cm^{-1}) = 3109, 3053, 2206 (CN), 2183 (CN), 1767, 1605, 1580, 1547, 1512, 1476, 1460, 1424, 1371, 1244, 1209, 1188, 1169, 1150, 893, 793.

Single crystals of (^{i}Pr$_2$fc)(TCNQ)$_2$ (**7**), (^{t}BuFc)(TCNQ)$_2$ (**8**), and (Me_2fc)(TCNQ)$_2$ (**9**)[11] were prepared as follows. A solution (4 mL) of the donor (0.10 mmol) and TCNQ (0.040 mmol) in acetonitrile (for **7**), acetone (for **8**) or CH_2Cl_2 (for **9**) was allowed to evaporate for 1–2 h under a reduced pressure. Black crystals precipitated, which were collected and washed with a minimum amount of acetone, and subjected to X-ray crystallography. In **8**, a small

amount of neutral TCNQ precipitated together with the salt, which was removed under a microscope. **7**: Yield: 33%. Anal. Calcd. for $C_{40}H_{30}FeN_8$ (678.56): C, 70.80; H, 4.46; N, 16.51. Found: C, 70.83; H, 4.44; N, 16.26 ν (cm^{-1}) = 3099, 2200 (CN), 2156 (CN), 1557, 1524, 1476, 1373, 1300, 1202, 1109, 1072, 1063, 1030, 951, 922. **8**: Yield: about 50%. Anal. Calcd. for $C_{38}H_{26}FeN_8$ (650.51): C, 70.16; H, 4.03; N, 17.23. Found: C, 70.08; H, 4.00; N, 17.21. ν (cm^{-1}) = 3107, 3049, 2978, 2199 (CN), 2176 (CN), 2158 (CN), 1593, 1557, 1524, 1483, 1416, 1337, 1321, 1304, 1275, 1204, 1190, 1134, 1117, 1076, 953, 872, 835, 822, 746. **9**: Yield: 57%. Anal. Calcd. for $C_{38}H_{26}FeN_8$ (622.46): C, 70.16; H, 4.03; N, 17.23. Found: C, 69.62; H, 3.49; N, 18.04. ν (cm^{-1}) = 3104, 2198 (CN), 2159 (CN), 1523, 1504, 1471, 1416, 1375, 1332, 1227, 1201, 1026, 980, 966, 830.

X-ray crystallography. X-ray diffraction data for single crystals were collected on a Bruker SMART APEX II CCD diffractometer using MoKα radiation (λ = 0.71073 Å). The crystal data, data collection parameters, and analysis statistics for these compounds are listed in Tables 1 and 2. All of the calculations were performed using SHELXL.[16] The structures were solved using the direct methods and expanded using Fourier techniques. ORTEP-3 for windows[17] was used for molecular graphics. The non-hydrogen atoms were refined anisotropically. Empirical absorption corrections were applied. The hydrogen atoms were inserted at the calculated positions and allowed to ride on their respective parent atoms.

CCDC 942241–942249 contains the supplementary crystallographic data for **1**–**9**. These data can be obtained free of charge from the Cambridge Crystallographic Data Centre via http://www.ccdc.cam.ac.uk/conts/retrieving.html.

Table 1. Crystallographic parameters for **1**–**4**.

	1	**2**	**3**	**4**
empirical formula	C24 H14 F4 Fe N4	C26 H18 F4 Fe N4	C26 H18 F4 Fe N4	C27 H20 F4 Fe N4
formula weight	490.24	518.29	518.29	532.32
crystal dimensions / mm^3	0.75×0.13×0.13	0.30×0.05×0.03	0.60×0.06×0.02	0.38×0.13×0.03
crystal system	Monoclinic	Monoclinic	Triclinic	Triclinic
a / Å	6.8456(5)	6.8934(6)	6.9080(9)	6.837(2)
b / Å	14.4051(10)	23.198(2)	12.2607(15)	11.958(3)
c / Å	20.8910(14)	13.9021(13)	15.056(3)	15.743(6)
α / deg			111.163(3)	67.695(5)
β / deg	103.566(3)	94.965(2)	98.851(3)	85.907(6)
γ / deg			96.721(2)	80.367(4)
V / Å	2002.6(2)	2214.7(3)	1154.3(3)	1174.0(6)
space group	$P2_1/c$	$P2_1/c$	*P*–1	*P*–1
Z value	4	4	2	2
ρ_{calcd} / g cm^{-3}	1.626	1.554	1.491	1.506
F (000)	992	1056	528	544
no. of reflections	14438	14243	6597	6139
no. of observations	4961	4539	4566	4242
parameters	397	322	344	328
temperature / K	173	173	173	90
$R_1{}^a$, $R_w{}^b$ ($I > 2\sigma$)	0.0474, 0.1320	0.0475, 0.1078	0.0554, 0.1269	0.0556, 0.1288
$R_1{}^a$, $R_w{}^b$ (all data)	0.0514, 0.1342	0.0714, 0.1184	0.0942, 0.1451	0.0937, 0.1463
goodness of fit	1.231	1.012	1.021	1.017

$^aR_1 = \Sigma||F_o| - |F_c|| \,/\, \Sigma|F_o|$. $^bR_w = [\Sigma w\,(F_o^2 - F_c^2)^2/\Sigma w\,(F_o^2)^2]^{1/2}$

Table 2. Crystallographic parameters for **5**–**9**.

	5	**6**	**7**	**8**	**9**
empirical formula	C38 H22 F4 Fe N8	C39 H24 F4 Fe N8	C40 H30 Fe N8	C38 H26 Fe N8	C36 H22 Fe N8
formula weight	722.49	736.51	678.57	650.52	622.47
crystal dimensions / mm^3	0.30×0.10×0.05	0.30×0.20×0.05	0.80×0.25×0.15	0.30×0.10×0.05	0.40×0.30×0.10
crystal system	Triclinic	Triclinic	Monoclinic	Triclinic	Triclinic
a / Å	8.7871(13)	8.8034(10)	6.6911(4)	7.625(2)	7.5255(6)
b / Å	12.7926(19)	12.8426(15)	15.5049(10)	14.563(4)	7.6535(6)
c / Å	15.286(2)	15.2449(17)	31.364(2)	28.821(7)	13.4176(11)
α / deg	90.751(3)	89.342(2)		86.928(3)	101.755(2)
β / deg	104.949(2)	76.634(2)	93.0530(10)	89.697(4)	93.869(2)
γ / deg	90.639(2)	89.102(2)		79.129(4)	94.593(2)
V / Å	1659.8(4)	1676.6(3)	3249.2(4)	3159.0(14)	751.38(10)
space group	*P*–1	*P*–1	$P2_1/c$	*P*–1	*P*–1
Z value	4	2	4	4	1
ρ_{calcd} / g cm^{-3}	1.446	1.459	1.387	1.368	1.376
F (000)	736	752	1408	1344	320
no. of reflections	9345	12365	19320	18110	5633

no. of observations	6464	8252	5996	11505	3679
parameters	500	472	447	1000	282
temperature / K	173	173	173	173	293
R_1[a], R_w[b] ($I > 2\sigma$)	0.0665, 0.1188	0.0574, 0.1121	0.0503, 0.1455	0.0683, 0.1204	0.0434, 0.1133
R_1[a], R_w[b] (all data)	0.1322, 0.1406	0.1429, 0.1438	0.0586, 0.11539	0.1627, 0.1572	0.0476, 0.1173
goodness of fit	0.999	0.948	1.177	0.940	1.062

[a] $R_1 = \Sigma||F_o| - |F_c|| / \Sigma|F_o|$. [b] $R_w = [\Sigma w (F_o^2 - F_c^2)^2/\Sigma w (F_o^2)^2]^{1/2}$

RESULTS AND DISCUSSION

General structural features. The structural determination of **1**–**9** revealed that the stoichiometries and the assembled structures of the alkylferrocenium salts with F_nTCNQ were strongly dependent on the acceptors. The F_4TCNQ salts **1**–**4** exhibited a D/A ratio of 1:1, whereas the F_2TCNQ salts **5**–**6** and the TCNQ salts **7**–**9** exhibited a D/A ratio of 2:1 (Chart 2). In these salts, F_4TCNQ was a monoanion, whereas the weaker acceptors F_2TCNQ and TCNQ adopted partial charges. In all of these salts, the donors and acceptors were stacked to form independent columns in the crystals. Salts **1**–**4** existed in a honeycomb-type hexagonal assembled structure of cation columns that surrounded the anion columns, as shown schematically in Figure 1a. The assembled structure closely resembles that of the alkylferrocenium salts with $[Ni(mnt)_2]$.[7] In contrast, salts **5**–**9** existed as rectangular arrangements of cation columns that surrounded the anion columns, as shown in Figure 1b. In the cation columns, the cations formed uniform stacks through intermolecular π–π interactions in the salts except for **5**, **6**, and **8**. In the acceptor columns, the F_4TCNQ in salts **1**–**4** formed diamagnetic dimers, whereas the F_2TCNQ and TCNQ in **5**–**9** exhibited only weak or no dimerization.

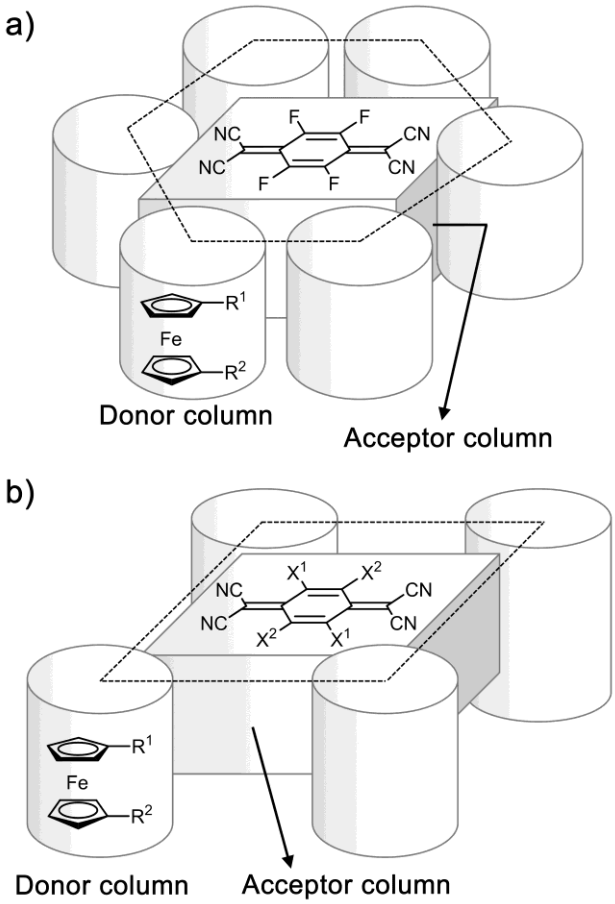

Figure 1. Schematic representation of the assembled structures of a) F_4TCNQ salts (**1**–**4**) and b) F_2TCNQ and TCNQ salts (**5**–**9**).

The general structural motifs of **1**–**9** consisted of columnar arrangements of the cations surrounding the anion columns, and their arrangements were dependent on the D/A ratios. This dependence of the D/A ratio occurred most likely as a consequence of the non-specific self-assembly of the donors and acceptors, and the comparable molecular sizes and stacking distances of the ferrocenes and the acceptors were most likely the key factors determining the structural characteristics of these structures. Indeed, the molecular volumes of the cations (Me_2fc: 224 Å^3, Et_2fc: 231 Å^3, ^{i}Pr$_2$fc: 267 Å^3, ^{t}BuFc: 228 Å^3, and ^{t}PeFc: 251 Å^3) were comparable to the acceptor volumes (F_4TCNQ: 224 Å^3, F_2TCNQ: 215 Å^3, and TCNQ: 206 Å^3). It is noteworthy that cations bearing similar substituents afforded similar packing

structures, as seen by the close resemblance of the structures of **1**, **3**, and **5** to those of **2**, **4**, and **6**, respectively (vide infra), although these structures were not isomorphous.

With regard to the local interactions between the cation and acceptor columns, the Fe atoms of the cations were commonly surrounded by two to four cyano groups from the acceptors. The Fe...N distances were 4.1–4.6 Å and therefore longer than the van der Waals distance because of the steric hindrance of the cations. The close Fe…N arrangements were probably resulted from steric factors rather than a direct interaction between the Fe and cyano groups, but they lead to a significant electrostatic interaction between the cations and anions because of the long range nature of the electrostatic force. Indeed, they were found to dominate the charge distributions on the acceptors in the F_2TCNQ and TCNQ salts **5**–**9**. Fe...NC- arrangements of this particular type have also been observed in the alkylferrocenium and biferrocenium salts with $[Ni(mnt)_2]$,[7,18] where they affected the valence states of these salts.

ORTEP drawings of the cations in these salts are shown in Figure S1 (Supporting information). The intramolecular Fe–C(Cp) distances were found to be 2.07–2.09 Å, which are typical values for ferrocenium cations.[19] Most of the cations exhibited disorder. The methyl groups of Me_2fc were disordered over two sites in **1** and four sites in **9**. One of the ethyl groups of Et_2fc in **2** exhibited 2-fold conformational disorder. The *tert*-butyl group of ^{t}BuFc in **3**, **7**, and **8** exhibited rotational disorder over two sites, and the unsubstituted Cp ring in **8** exhibited 2-fold rotational disorder.

The arrangements of the cations and anions, intermolecular distances, and charge distributions on the acceptors in **1**–**9** are summarized in Table 3. The structures and valence states of the different salt will be described in detail in the following sections.

Table 3. Molecular arrangements and intermolecular distances.

compound		cation arrangement	Cp...Cp[a] / Å	charge on acceptor	acceptor arrangement	TCNQ...TCNQ[c] / Å
1:1 salts	(Me_2fc)(F_4TCNQ) (**1**)	regular 1D	3.449	−1	dimer	3.278, 3.573
	(Et_2fc)(F_4TCNQ) (**2**)	regular 1D	3.504	−1	dimer	3.256, 3.648
	(^{t}BuFc)(F_4TCNQ) (**3**)	regular 1D	3.738	−1	dimer	3.298, 3.949
	(^{t}PeFc)(F_4TCNQ) (**4**)	regular 1D	3.661	−1	dimer	3.298, 3.868
1:2 salts	(^{t}BuFc)(F_2TCNQ)$_2$ (**5**)	dimer	3.802	−0.63, −0.48	tetramer	3.397, 3.787
	(^{t}PeFc)(F_2TCNQ)$_2$ (**6**)	dimer	3.807	−0.41, −0.45	dimer	3.403, 3.862
	(^{i}Pr$_2$fc)(TCNQ)$_2$ (**7**)	regular 1D	3.289	−0.66, −0.25	dimer	3.892, 4.002
	(^{t}BuFc)(TCNQ)$_2$ (**8**)	tetramer	3.476, 3.747	−0.23, −0.63, −0.29, −0.26	tetramer	3.742, 3.747, 3.749, 3.790
	(Me_2fc)(TCNQ)$_2$ (**9**)	regular 1D	4.662	−0.75, −0.30	regular 1D	3.827

[a]Intermolecular distances between the centroids of Cp rings. [b]The charges for F_2TCNQ and TCNQ were estimated from the bond lengths (Ref. 20). [c]Intradimer and interdimer distances between the centroids of the quinoid rings of TCNQ.

Structures of the F_4TCNQ salts. Salts **1**−**4** exhibited a D/A ratio of 1:1, and the cation columns constituted a hexagonal arrangement (Figure 1a). The packing diagrams of **1**–**2** and **3**–**4** are shown in Figures 2 and 3, respectively. The packing structure of **1** resembled that of **2**, whereas the packing structure of **3** resembled that of **4**, and these resemblances were attributed to the similar shapes of the cations. One donor and one acceptor molecule were crystallographically independent in each salt. The cations formed uniform stacking interactions in the column through π–π contacts between the Cp rings, as shown in Figure 4a. The deviation from linear stacking was greater for **3** and **4** as a consequence of steric hindrance between the cation substituents. The columnar stacking of the anions in **1**–**4** is shown in Figure 4b. The anions form dimers in the columns, and the intradimer overlap integrals (S_1 = 2.2–2.7×10^{-2}) were about twice the size of the interdimer values (S_2 = 1.2–1.3×10^{-2}). The dimers were uniformly stacked in **1** and **2**, but were shifted in **3** and **4** along the molecular long axes because of the substituents on the cation. With regard to the local

interactions between the cations and anions, four cyano groups surrounded the Fe atoms in **1** (Fe...N distances: 4.1–4.4 Å), three cyano groups surrounded the Fe atoms in **2** and **3** (Fe...N distances: 4.1–4.4 Å for **2**, and 4.2–4.6 Å for **3**), and only two cyano groups surrounded the Fe atoms in **4** (Fe...N distances:4.3 and 4.4 Å).

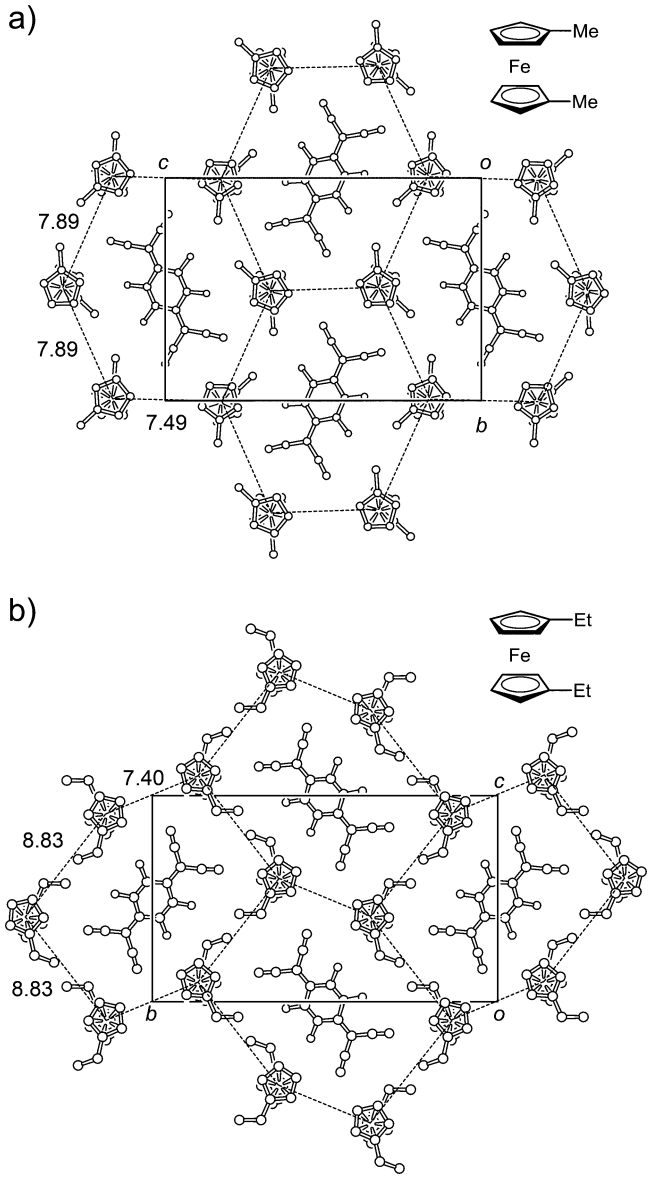

Figure 2. Packing diagrams of a) (Me_2fc)(F_4TCNQ) (**1**) and b) (Et_2fc)(F_4TCNQ) (**2**) viewed along the stacking axes. The intercolumnar Fe…Fe distances (Å) are indicated by the dashed lines.

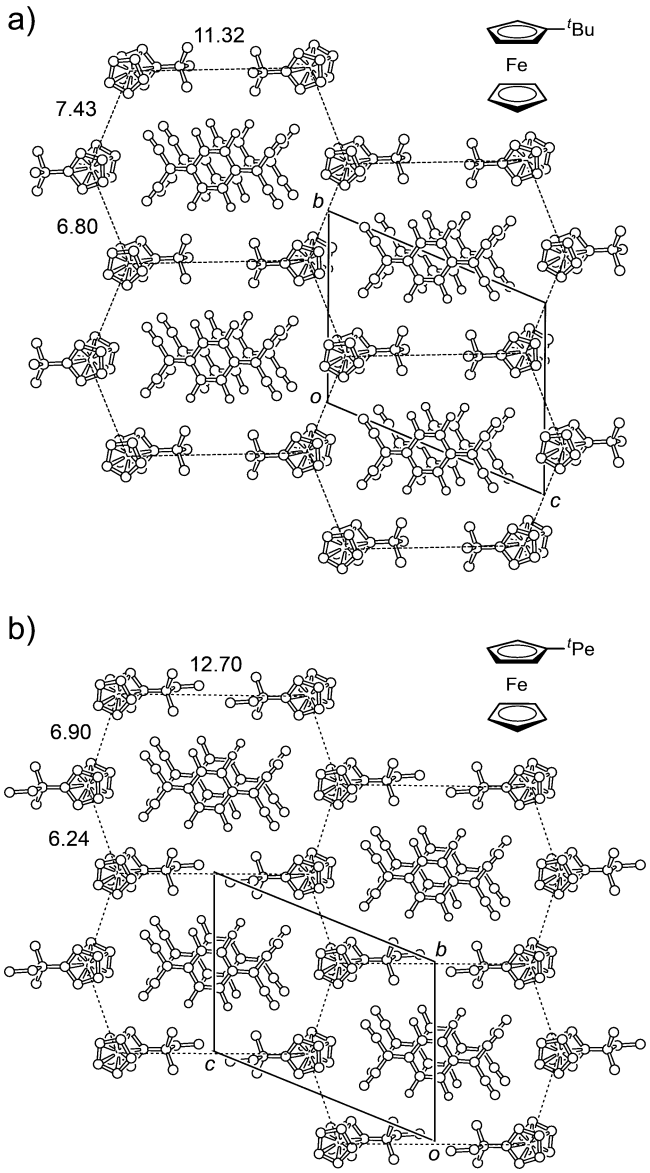

Figure 3. Packing diagrams of a) (^{t}BuFc)(F_4TCNQ) (**3**) and b) (^{t}PeFc)(F_4TCNQ) (**4**) viewed along the stacking axes. The intercolumnar Fe…Fe distances (Å) are indicated by the dashed lines.

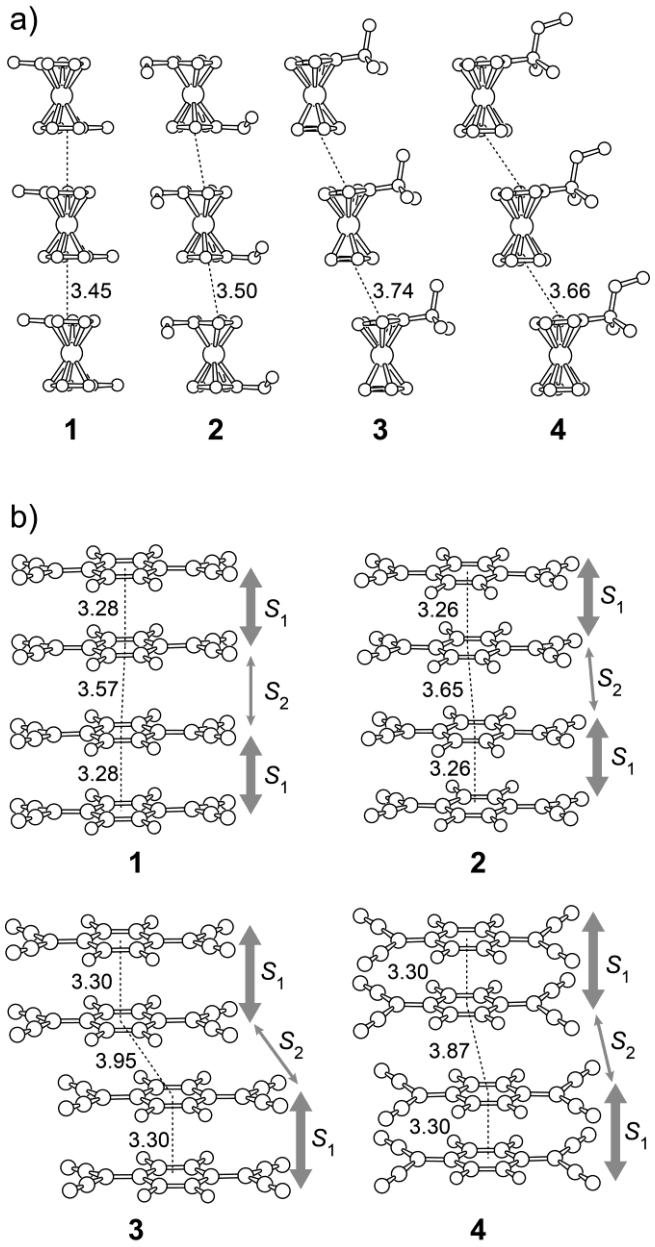

Figure 4. a) Donor arrangements and b) acceptor arrangements in (Me_2fc)(F_4TCNQ) (**1**), (Et_2fc)(F_4TCNQ) (**2**), (^{t}BuFc)(F_4TCNQ) (**3**), and (^{t}PeFc)(F_4TCNQ) (**4**). The intermolecular centroid–centroid distances are indicated by the dashed lines. Definitions of the overlap integrals (S_1, S_2) are shown by the arrows in b) (see text).

The hexagonal assembled structure was also seen in the alkylferrocenium salts of [M(mnt)$_2$]. [Ni(mnt)$_2$] often exhibits intermolecular S…S interactions and usually affords different packing structures from those of the TCNQ derivatives. Both of these acceptors,

however, are cyano acceptors that adopt a −1 charge, and possess comparable molecular volumes (F_4TCNQ: 224 Å^3 and [Ni(mnt)$_2$]: 231 Å^3), as well as forming stacking arrangements. Taken together, these factors probably lead to the common assembled structures. Salts **2** and **3**, in particular, were almost isomorphous with the corresponding [Ni(mnt)$_2$] salts consisting of the same cations. This architecture was therefore proven to be one of the general structural types for metallocenium complexes. [D_2][{M(mnt)$_2$}$_2$] (D = FeCp*$_2$, CoCp$_2$) also exhibit similar structures.[6a]

Structures of F_2TCNQ and TCNQ salts. Salts **5**–**9** all had a D/A ratio of 1:2, and the cation columns exhibited a rectangular arrangement (Figure 1b). One donor and two acceptor molecules were crystallographically independent in each salt except for **8**.

The packing diagram of **6** is shown in Figure 5. The cations formed dimers *via* the Cp...Cp contacts in the column. In the acceptor column, the molecules form dimers, which were further paired to form tetramers. The intradimer overlap integral (S_1 = 1.78 × 10^{-2}) was about twice that of the interdimer value (S_2 = 8.13 × 10^{-3}) in the tetramer. It was therefore anticipated that the tetramer would have two spins located on each dimer. The interactions between the tetramers were small, with centroid–centroid distances greater than 5 Å and small overlap integrals (7.84×10^{-4} and 3.86×10^{-4}). The formal charges on acceptors A and B were estimated from the bond lengths[20] to be –0.45 and –0.41, which were virtually −0.5, considering the margin for errors. One cyano group was found to be close to the Fe atom of the cation in each acceptor (Fe…N distance: 4.4 Å). The packing structure of **5**, bearing a ^{t}Bu group instead of ^{t}Pe group in the cation, was almost identical to that of **6** (Figure S2, Supporting information). The negative charge distributions on the acceptors were –0.63 and –0.48. Each acceptor had one Fe...NC- interaction (Fe...N distances: 4.4 Å and 4.5 Å), and the larger negative charge distribution on the former molecule was consistent with its shorter Fe...CN- distance.

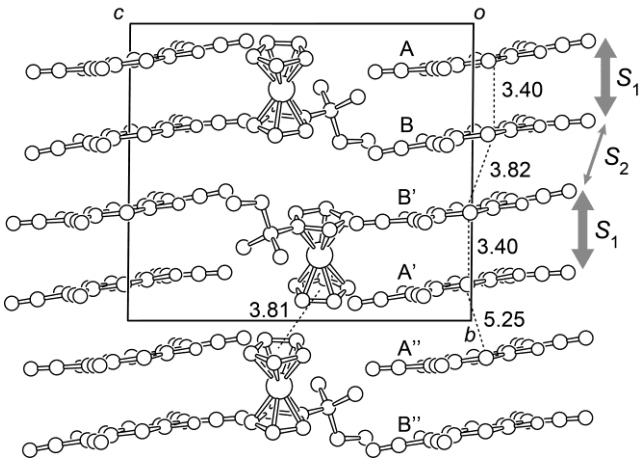

Figure 5. Packing diagram of (^{t}PeFc)(F_2TCNQ)$_2$ (**6**). The definitions of the overlap integrals are indicated by the arrows.

The packing diagram of **7** is shown in Figure 6a. The donors were stacked uniformly through short Cp...Cp contacts (centroid–centroid distance: 3.289 Å), which were shorter than those in the other salts (3.449 Å–3.807 Å). The interplanar distance between the Cp rings was 3.282 Å, and was therefore shorter than the usual π–π intermolecular distance of 3.4–3.6 Å. The acceptors were stacked into columns in such a way that the molecules had effectively slipped alternately along the molecular long axes because of the steric hindrance of the cation (Figure 6b). The acceptor molecules were found to be only weakly dimerized in the column, and the overlap integrals were nearly comparable (S_1 = 1.49 × 10^{-2} and S_2 = 1.26 × 10^{-2}). Of the two crystallographically independent TCNQ molecules, only molecule A had its two cyano groups close to the Fe atom (Fe…N distances: 4.0 Å and 4.3 Å). The formal charges of molecules A and B were estimated from the bond lengths to be –0.66 and –0.25, respectively. The larger negative charge distribution on the former molecule was attributed to the stronger interaction with the cation. The structure of this salt closely resembled that of **9**[11], which had Me groups instead of ^{i}Pr groups in the cation (Figure S3). The two acceptor molecules had charges of −0.75 and −0.30. The former molecule was close to the cation (Fe…N distance:

4.1 Å), which accounted for its larger negative charge.[11] The acceptors formed uniform stacking interactions, and exhibited no dimerization.

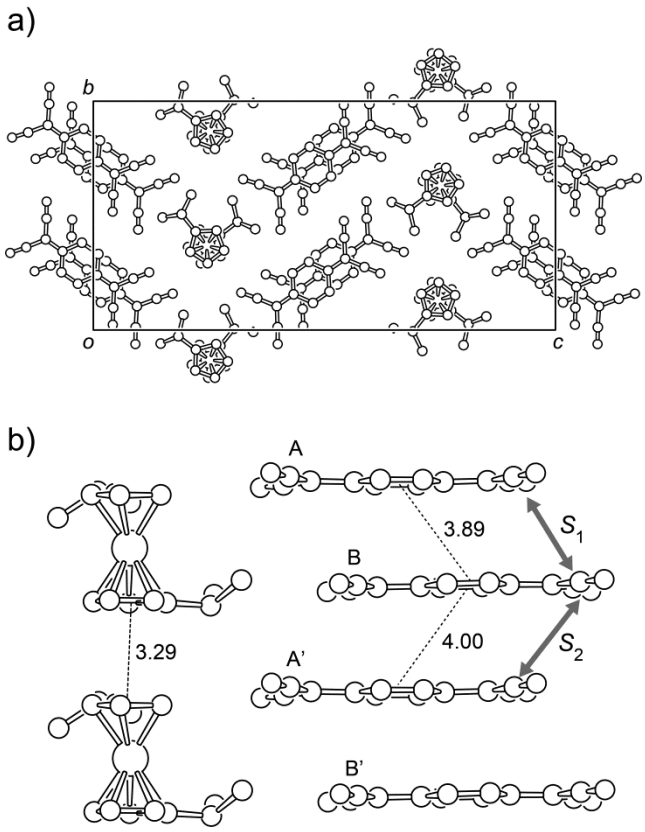

Figure 6. a) Packing diagram and b) molecular arrangements of (^{i}Pr$_2$fc)(TCNQ)$_2$ (**7**). The intermolecular centroid–centroid distances are indicated by the dashed lines. The definitions of the overlap integrals are shown by the arrows.

The packing diagram of **8** is shown in Figure 7. This salt was exceptional in that two of the cations and four of the acceptors (A–D) were crystallographically independent. The cations and the acceptors both formed tetramer structures in the columns. In the anion columns, the overlap integrals in the tetramers (A–D) were 1.60–1.93×10^{-2}, whereas those between the tetramers were smaller at 3.96–9.50×10^{-3}. The Fe atoms in the cation were surrounded by four cyano groups. The negative charges on molecules A–D were estimated from the bond lengths to be –0.23, –0.63, –0.29, and –0.26, respectively. The charge distribution on molecule B was large, and therefore consistent with there being three cyano

groups surrounding the Fe atom (Fe…N distances: 4.2–4.5 Å), whereas molecules A and C only had one groups of this type (Fe…N distances: 4.4 Å). Molecule D, however, had small negative charge density despite having three such interactions (4.2–4.5 Å). The reason for this disparity remains unclear but could be related to interactions with other acceptors. The structures of **5** and **8** were different, although both salts possessed the same cation (^{t}BuFc) and the same D/A ratio of 1:2.

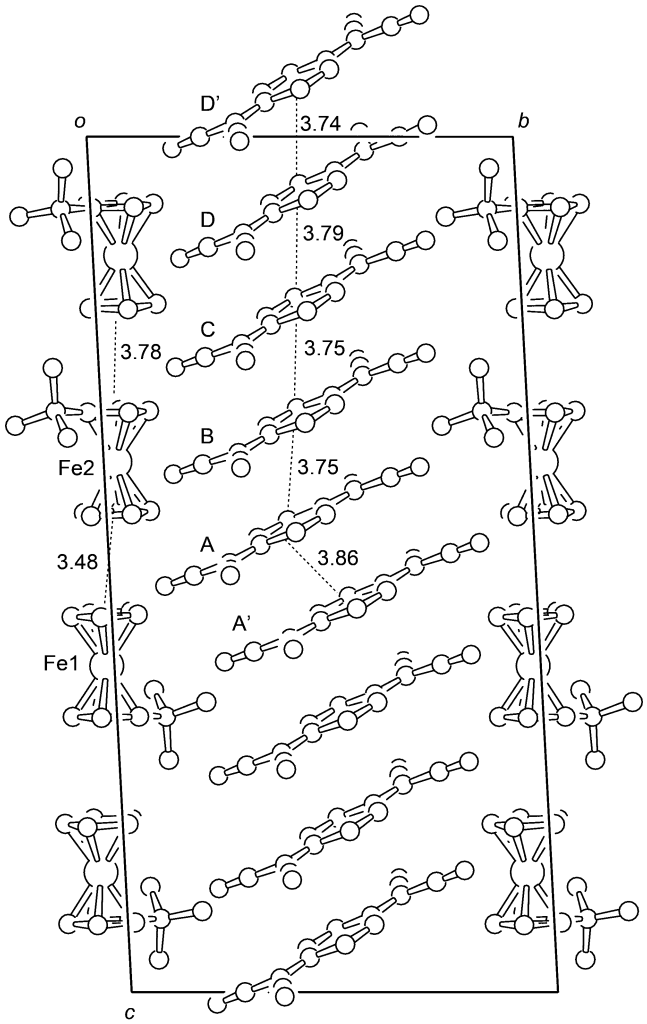

Figure 7. Packing diagram of (^{t}BuFc)(TCNQ)$_2$ (**8**) projected along the *a*-axis. The intermolecular centroid–centroid distances are indicated by the dashed lines.

Magnetic susceptibilities. The temperature dependences of the magnetic moments of **1**–**3** are shown in Figure 8a. These salts exhibited simple paramagnetic behaviors. The χT

values for **1**, **2**, and **3** at ambient temperature were 0.60, 0.70, and 0.71 emu K mol^{-1}, respectively. These values corresponded well with the contribution of the ferrocenium cations, as expected from the dimerization of the F_4TCNQ anions. The χT values were almost temperature independent, and gradually decreased below 85 K. The antiferromagnetic interactions between the cations were estimated through the fitting of the susceptibilities using the Bonner–Fisher model,[21] considering the regular one-dimensional arrangement of the cations. The J/k_B values determined for **1**–**3** were −2.6, −1.2, and −0.8 K, respectively. The g value derived from the fitting was 2.65. Another potential reason for the observed reductions in the magnetic moments at low temperatures could be a reduction in the orbital contribution.[22]

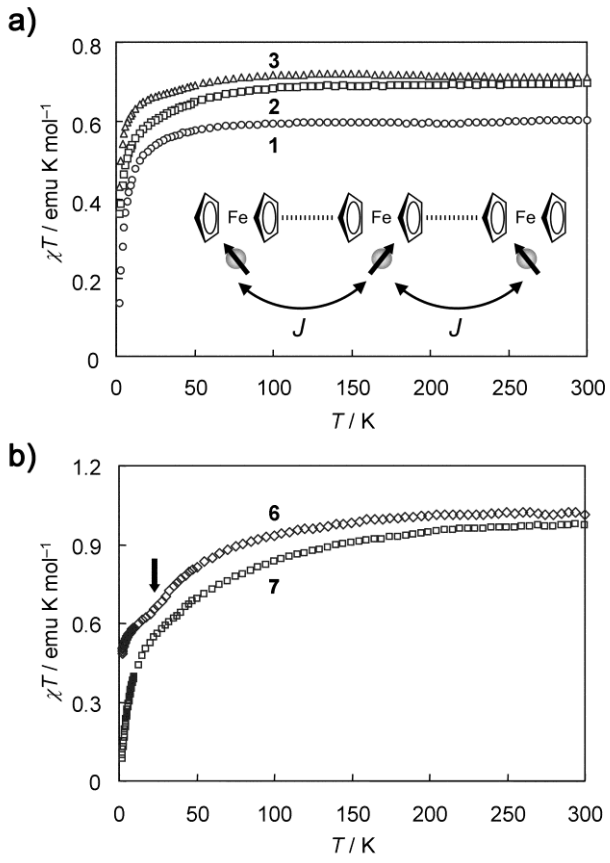

Figure 8. Temperature dependence of the magnetic moments of a) (Me_2fc)(F_4TCNQ) (**1**), (Et_2fc)(F_4TCNQ) (**2**), and (^{t}BuFc)(F_4TCNQ) (**3**), and b) (^{t}PeFc)(F_2TCNQ)$_2$ (**6**) and (^{i}Pr$_2$fc)(TCNQ)$_2$ (**7**). The arrow in b) indicates the inflection point for **6** (see text).

The temperature dependences of the magnetic moments of **6** and **7** are shown in Figure 8b. The χT values at ambient temperature were 1.01 and 0.98 emu K mol^{-1}, respectively. These values corresponded well with the sum of the iron spin on the cation and the spin on the acceptor dimer (0.375 emu K mol^{-1}), and are therefore consistent with the crystal structures. In **6**, the χT value decreases below 100 K, showing an inflection point at around 25 K. The χT value at this temperature was about 0.7 emu K mol^{-1}, which corresponded well with the value of the ferrocenium cation. Heat capacity measurements revealed the presence of a phase transition at around 34 K (Figure 9), which most likely corresponded to the singlet formation of the acceptor spins. The phase transition entropy was 5.2 J mol^{-1} K^{-1}, which is comparable to the expected value for singlet formation (R ln 2 = 5.7 J mol^{-1} K^{-1}). In **7**, the χT value was gradually reduced at low temperatures, and no anomalies were detected by the specific heat measurements.

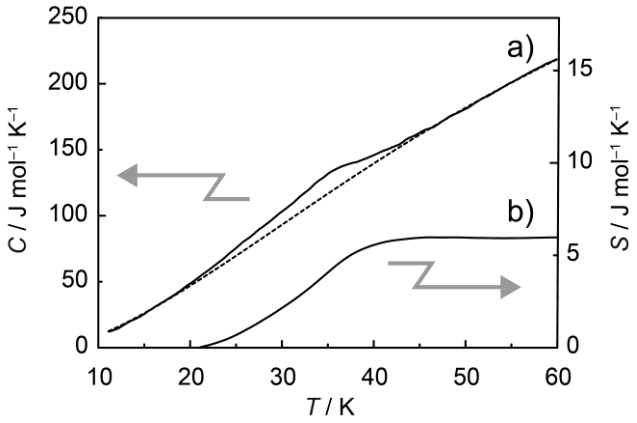

Figure 9. a) Molar heat capacity and b) excess entropy of **6**. The dashed line in a) represents the estimated lattice contribution.

The magnetic susceptibilities at low temperatures were dominated by the cation spins. Of the salts investigated in the current study, the temperature dependence of the magnetic susceptibility of **1** and **7** exhibited maxima at 3.0 K and 4.2 K, respectively, whereas the other salts did not exhibit such maxima. These results suggested that **1** and **7**, which had shorter

Cp...Cp distances than the other salts, possessed larger antiferromagnetic interactions than the other salts. Figure 10 shows the χT values of the salts at 2 K plotted as function of the Cp…Cp distance. The values clearly became smaller as the Cp…Cp distance was reduced, suggesting an increase in the antiferromagnetic interactions. We previously reported the precise determination of the antiferromagnetic interaction via the Cp...Cp contact in (^{n}BuFc)[Ni(mnt)$_2$] (J = 2.5 K, based on singlet-triplet model) using calorimetric measurements.[7] The shorter Cp...Cp distance in **7** (3.289 Å) compared with (^{n}BuFc)[Ni(mnt)$_2$] (3.317 Å) most likely resulted in the smaller χT value of the salt at 2 K (**7**: 0.087 emu mol^{-1}, (^{n}BuFc)[Ni(mnt)$_2$]: 0.288 emu mol^{-1}).

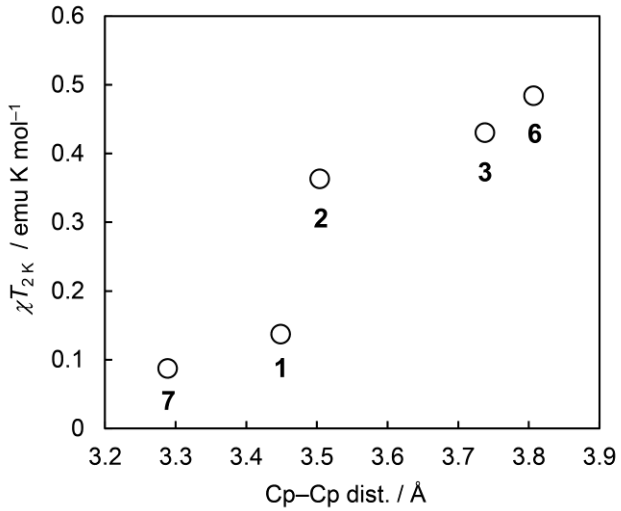

Figure 10. χT values at 2 K plotted as a function of the intermolecular Cp...Cp distances in the salts.

CONCLUSION

The D/A ratios of the alkylferrocenium salts with F$_n$TCNQ were found to be dependent on the acceptors. F$_4$TCNQ gave 1:1 salts, whereas F$_2$TCNQ and TCNQ produced 1:2 salts. The cation columns were arranged in a hexagonal manner for the 1:1 D/A salts, whereas the 1:2 D/A salts were arranged in a rectangular manner. The differences in these arrangements

occurred as a consequence of the nonspecific self-assembly of the donors and acceptors. The comparable molecular sizes and stacking distances of the ferrocenes and the acceptors appeared to be critical factors for determining these structures. The cation shape did not affect the packing structures. The donor–acceptor interactions of the Fe...NC- arrangement dominated the charge distribution on the acceptors. Antiferromagnetic interactions of less than a few Kelvin operated via the Cp…Cp contacts. (^{i}Pr$_2$fc)(TCNQ)$_2$ exhibited the shortest Cp...Cp distance, and showed the smallest magnetic moment at low temperatures of all of the salts tested in the current study.

AUTHOR INFORMATION

Corresponding Author

E-mail: tmochida@platinum.kobe-u.ac.jp; tel/fax: +81-78-803-5679.

Notes

The authors declare no competing financial interest.

ACKNOWLEDGMENT

This work was financially supported by KAKENHI (Grant nos. 23110719 and 17685003). This work was performed using the facilities of the Institute for Solid State Physics at The University of Tokyo.

Supporting Information

ORTEP drawings of the molecular structures of the cations in **1**–**9**, packing diagrams of **5** and **9**. X-ray crystallographic information files are available for **1**–**9**.

REFERENCES

(1) (a) Haiduc, I.; Edelmann, F.T. *Supramolecular Organometallic Chemistry*, Willey-VCH, Weinheim, 1999; (b) *Comprehensive Supramolecular Chemistry*; Lehn, J.-M., Atwood, J. L., Davis, J. E. D., MacNicol, D. D., Vögtle, F., Eds.; Pergamon Press: Oxford, 1990–1996; Vol. 1–11; (c) *The Crystal as a Supramolecular Entity*; Desiraju, G. R., Ed.; Perspectives in Supramolecular Chemistry; Wiley, Chichester, 1996, Vol. 2. (d) Janiak, C. *Dalton Trans.* **2003**, 2781–2804.

(2) (a) Braga, D.; Grepioni, F.; Desiraju, G. R. *Chem. Rev.* **1998**, *98*, 1375–1406; (b) Braga, D.; Brammer, L.; Champness, N. R. *CrystEngComm* **2005**, *7*, 1–19; (c) Braga, D.; Maini, L.; Polito, M.; Scaccianoce, L.; Cojazzi, G.; Grepioni, F. *Coord. Chem. Rev.* **2001**, *216–217*, 225–248.

(3) (a) Horikoshi, R. *Coord. Chem. Rev*. **2013**, *257*, 621–637; (b) Horikoshi, R.; Mochida, T. *Eur. J. Inorg. Chem.* **2010**, *34*, 5355–5371; (c) Mochida, T.; Shimuzu, F.; Shimizu, H.; Okazawa, K.; Sato, F.; Kuwahara, D. *J. Organomet. Chem.* **2007**, *692*, 1834–1844.

(4) (a) *Ferrocenes: Homogenous Catalysis, Organic Synthesis, Materials Science*; Togni, A., Hayashi, T., Eds.; Wiley–VCH: Weinheim, 1995, Chapter 8. (b) Long, N. J.; *Metallocenes: an introduction to sandwich complexes*, Blackwell Science: Oxford, 1998.

(5) (a) Miller, J. S.; Epstein, A. J.; Reiff, W. M. *Angew. Chem. Int. Ed. Engl*. **1994**, *33*, 385–415; (b) Miller, J. S.; Epstein, A. J.; Reiff, W. M. *Chem. Rev*. **1988**, *88*, 201–220; (c) Quazi, A.; Reiff, W. M.; Kirss, R. U. *Hyperfine Interact*. **1994**, *93*, 1597–1603; (d) Zürcher, S.; Petrig, J.; Gramlich, V.; Worle, M.; Mensing, C.; von Arx, D.; Togni, A. *Organometallics*, **1999**, *18*, 3679–3689.

(6) (a) Bellamy, D.; Connelly, N. G.; Lewis R. G.; Orpen, A. G. *CrystEngComm* **2002**, *4*, 51–58; (b) Faulmann, C.; Cassoux, P. *Prog. Inorg. Chem*. **2004**, *52*, 399–489.

(7) Mochida, T.; Koinuma, T.; Akasaka, T.; Sato, M.; Nishio, Y.; Kajita, K.; Mori, H. *Chem. Eur. J*. **2007**, *13*, 1872–1881.

(8) Pac, S. -S.; Saito, G. *J. Solid State Chem.* **2002**, *168*, 486–496.

(9) (a) Hasegawa, T.; Inukai, Y.; Kagoshima, S.; Sugawara, T.; Mochida, T.; Sugiura, S.; Iwasa, Y. *Synth. Met*. **1997**, *86*, 1801–1802; (b) Hasegawa, T.; Kagoshima, S.; Mochida, T.; Sugiura, S.; Iwasa, Y. *Solid State Commun*. **1997**, *103*, 489–493.

(10) Mochida, T.; Yamazaki, S.; Suzuki, S.; Shimizu, S.; Mori, H. *Bull. Chem. Soc. Jpn.* **2003**, *76*, 2321–2328.

(11) Wilson, S. R.; Corvan, P. J.; Seiders, R. P.; Hodgson, D. J.; Brookhart, M.; Hatfield, W. E.; Miller, J. S.; Reis, Jr., A. H.; Rogan, P. K.; Gebert, E.; Epstein, A. J. *NATO Conference Series VI: Materials Science*, **1979**, *1*, 407–414.

(12) Mori, T.; Kobayashi, A.; Sasaki, Y.; Kobayashi, H.; Saito, G.; Inokuchi, H. *Bull. Chem. Soc. Jpn.* **1984**, *57*, 627–633.

(13) *Spartan '10*; Wavefunction, Inc.: Irvine, CA, 2011.

(14) Matsui, A.; Takaoka, Y.; Nishio, Y.; Kato, R.; Kajita, K. *J. Phys.: Conf. Ser.* **2009**, *150*, 042120.

(15) Mochida, T.; Hasegawa, T.: Kagoshima, S.; Sugiura, S.; Iwasa, Y. *Synth. Met*. **1997**, *86*, 1797–1798.

(16) Sheldrick, G. M. *SHELXL, Program for the Solution of Crystal Structures*; University of Göttingen: Göttingen, Germany, 1997.

(17) ORTEP-3 for Windows: Farrugia, L. J. *J. Appl. Cryst*. **1997**, *30*, 565.

(18) Mochida, T.; Takazawa, K.; Matsui, H.; Takahashi, M.; Takeda, M.; Sato, M.; Nishio, Y.; Kajita, K.; Mori, H. *Inorg. Chem*. **2005**, *44*, 8628–8641.

(19) Mammano, N. J.; Zalkin, A.; Landers, A.; Rheingold, A. L. *Inorg. Chem*. **1977**, 16, 297–300.

(20) Kistenmacher, T. J.; Emge, T. J.; Bloch, A. N.; Cowan, D. O. *Acta Cryst*. **1982**, *B38*, 1193–1199.

(21) Bonner, J. C.; Fisher, M. E. *Phys. Rev.* **1964**, *135*, A640–A658.

(22) Hendrickson, D. N.; Shon, Y. S.; Gray, H. B. *Inorg. Chem*. **1971**, *10*, 1559–1563.

For Table of Contents Use Only

Crystal Architectures and Magnetic Properties of Alkylferrocenium salts with F_nTCNQ (n = 0, 2, 4): Effect of Substituents on the Assembled Structures

Tomoyuki Mochida,*[,†,‡] Takahiro Akasaka,[†,‡] Yusuke Funasako,[†] Yutaka Nishio,[§] and Hatsumi Mori[¶]

SYNOPSIS. The crystal architectures of the alkylferrocenium salts of F_nTCNQ have been investigated. The F_4TCNQ salts had a 1:1 D/A stoichiometry, and existed as hexagonal honeycomb-like assembled structures of cation columns surrounding anion columns. The salts of F_2TCNQ and TCNQ had a D/A ratio of 1:2, and existed as rectangular arrangements of the cation columns. Weak antiferromagnetic interactions operate between the cations in these salts.

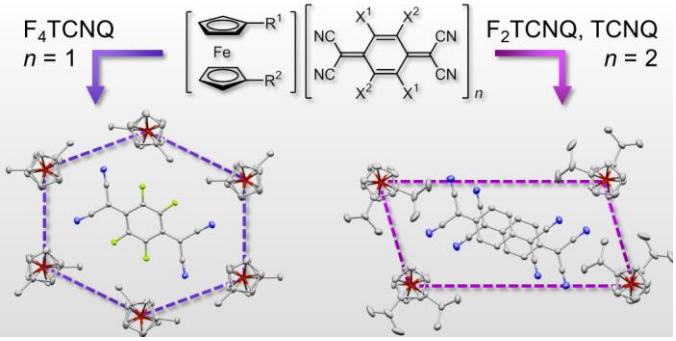

Supporting Information

Crystal Architectures and Magnetic Properties of Alkylferrocenium salts with F_nTCNQ (n = 0, 2, 4): Effect of Substituents on the Assembled Structures

Tomoyuki Mochida,*[,†,‡]Takahiro Akasaka,[†,‡] Yusuke Funasako,[†] Yutaka Nishio,[§] and Hatsumi Mori[¶]

[†]*Department of Chemistry, Graduate School of Science, Kobe University, Kobe, Hyogo 657-8501, Japan*

[‡]*Department of Chemistry, Faculty of Science, Toho University, Miyama, Funabashi, Chiba 274-8510, Japan*

[§]*Department of Physics, Faculty of Science, Toho University, Miyama, Funabashi, Chiba 274-8510, Japan*

[¶]*Institute for Solid State Physics, The University of Tokyo, Kashiwanoha, Kashiwa, Chiba 277-8581, Japan*

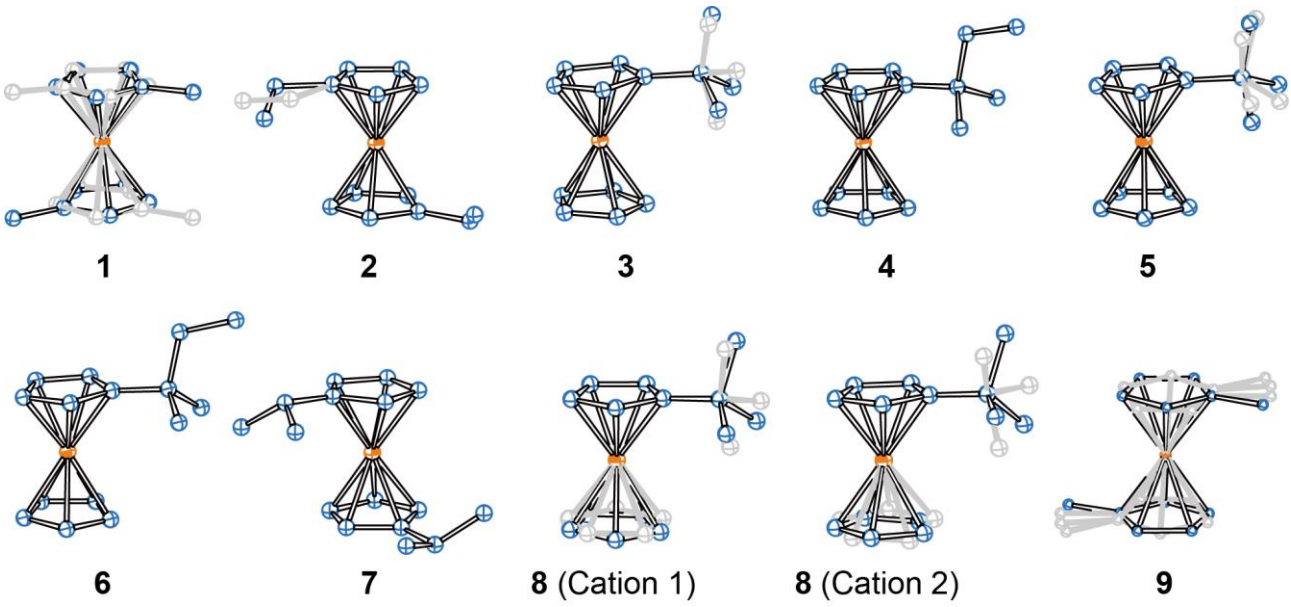

Figure S1. ORTEP drawings of the cations in **1**–**9**. The hydrogen atoms have been omitted for clarity. One of the disordered components in each molecule is represented in gray.

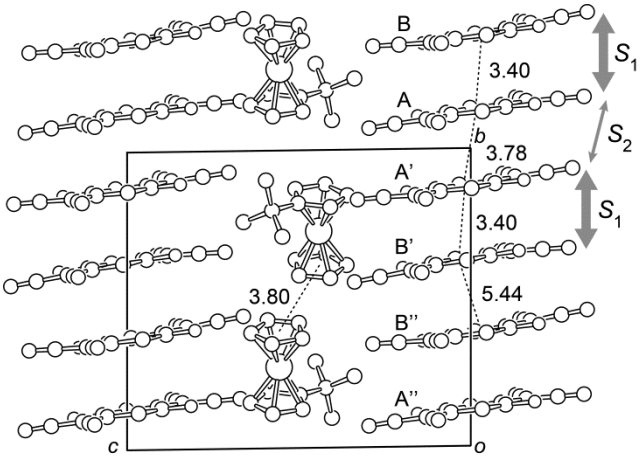

Figure S2. Packing diagram of (^{t}BuFc)(F_2TCNQ)$_2$ (**5**). The intermolecular centroid–centroid distances (Å) are indicated by the dashed lines. The definitions of the overlap integrals (S_1, S_2) are shown.

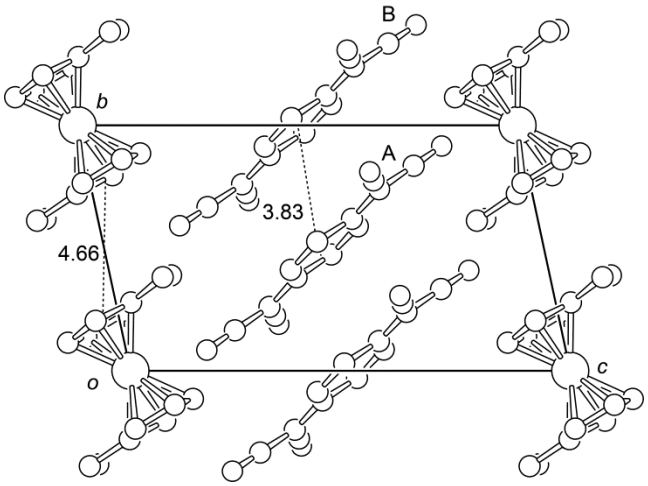

Figure S3. Packing diagram of (Me_2fc)(TCNQ)$_2$ (**9**). The intermolecular centroid–centroid distances (Å) are indicated by the dashed lines.